Fast Estimation Technology of Orbit Information for Non-cooperative Space Targets Based on AREKF Filtering Theory

Zhuo Zhang[1,2(✉)], Gang Liu[1], Henghai Fan[2], Dongmei Kuang[2], Anliang Li[2], and Ruixi Gaoya[2]

[1] School of Nuclear Engineering, Rocket Force Engineering University, Xi'an, China
zhangzhuozjb@163.com
[2] China Xi'an Satellite Control Center, Xi'an, People's Republic of China

Abstract. Based on the on-orbit acquisition of non cooperative targets, this paper establishes attitude and orbit coupling dynamic model, considering the relative motion uncertainty and measurement error under maneuvering conditions, then, Based on the principle of AREKF filter, a fast estimation method for the orbit information of non cooperative goal is proposed. This article provides a good estimate of the relative location, speed and posture of two satellites. Relative location estimation error is 0.4 m, relative speed is 0.002 m/s, and the relative attitude control precision is above 1°.

Keywords: Non-cooperative space target · Relative motion model · AREKF filtering · Fast estimation of orbit information

1 Introduction

Non-cooperative space target manipulation is a new project for space security maintenance. Advanced non-cooperative space target manipulation technology can not only effectively extend the service life of future spacecraft, improve on-orbit services, but also get a more economical, environmental friendly and competitive industrial process, which makes non-cooperative space target manipulation technology a hot spot in space technology research [1–3].

With the increasing demand for non-cooperative space target on-orbit acquisition and approach reconnaissance, a lot of countries have conducted in-depth research on the theory of non-cooperative target manipulation in space, such as module replacement, fuel injection, approach and acquisition, which include the orbit correction spacecraft (SUMO) [4], the autonomous rendezvous demonstration technology (DART) and the experimental small satellite (XSS) of the United States [5] etc. (Figs. 1 and 2).

2 Modeling and Analysis of Relative Motion of Non-cooperative Target

In the case of uncooperative target, the lack of relative position marker, can only rely on autonomous sensors to obtain the measurement method, the relative location-posture

© The Author(s), under exclusive license to Springer Nature Singapore Pte Ltd. 2023
Y. Wang et al. (Eds.): ICSINC 2022, LNEE 996, pp. 179–185, 2023.
https://doi.org/10.1007/978-981-19-9968-0_22

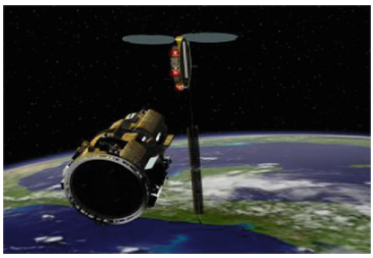

Fig. 1. SUMO refueling

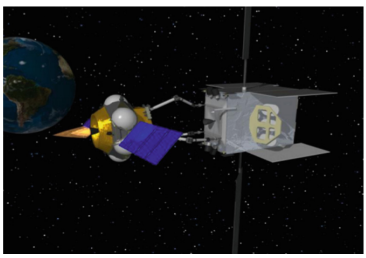

Fig. 2. DART tracking satellite and target satellite

equation of two satellites are established, which provides a mathematical basis for the next step of ultra-close relative motion tracking and control of non-cooperative targets [6].

Orbit coupling dynamic model of target satellite and tracking Satellite are

$$\begin{aligned}
&\dot{\boldsymbol{r}}_t = \boldsymbol{v}_t, \dot{\boldsymbol{v}}_t = \boldsymbol{g}_t + \boldsymbol{a}_t + \boldsymbol{w}_{gt} && \dot{\boldsymbol{r}}_c = \boldsymbol{v}_c, \dot{\boldsymbol{v}}_c = \boldsymbol{g}_c + \boldsymbol{w}_{gc}, \quad (\boldsymbol{v}_c)^{+c} = (\boldsymbol{v}_c)^{-c} + \boldsymbol{u}_{\Delta v} \\
&\dot{\boldsymbol{q}}_{i\to t} = \frac{1}{2}\boldsymbol{\omega}_t^t \otimes \boldsymbol{q}_{i\to t} && \dot{\boldsymbol{q}}_{i\to c} = \frac{1}{2}\boldsymbol{\omega}_c^c \otimes \boldsymbol{q}_{i\to c} \\
&\dot{\boldsymbol{\omega}}_t^t = \boldsymbol{I}_t^{-1}\left[\boldsymbol{\tau}_g^t - \boldsymbol{\omega}_t^t \times \left(\boldsymbol{I}_t\boldsymbol{\omega}_t^t\right)\right] + \boldsymbol{w}_{\alpha t} && \dot{\boldsymbol{\omega}}_c^c = \boldsymbol{I}_c^{-1}\left[\boldsymbol{u}_\tau^c + \boldsymbol{\tau}_g^c - \boldsymbol{\omega}_c^c \times \left(\boldsymbol{I}_c\boldsymbol{\omega}_c^c\right)\right] + \boldsymbol{w}_{\alpha c}
\end{aligned} \tag{1}$$

The relative position vector of the tracking satellites σ = rc-rt, and the vector form of the nonlinear relative motion dynamics model can be obtained [7]:

$$\frac{d^2\boldsymbol{\sigma}}{dt} = -\dot{\Omega}_{\mathbf{t}} \times \boldsymbol{\sigma} - 2\boldsymbol{\Omega}_t \times \dot{\sigma} - \boldsymbol{\Omega}_t \times (\boldsymbol{\Omega}_{\mathbf{t}} \times \boldsymbol{\sigma}) + \frac{\mu}{r_t^3}\left[\boldsymbol{r}_t - \left(\frac{r_t}{r_c}\right)^3 \boldsymbol{r}_c\right] + \Delta\boldsymbol{f}_d + a_c - a_t \tag{2}$$

where $\boldsymbol{\Omega}_{\mathbf{t}}$ represents the orbital angular speed. Then

$$\begin{cases}
\ddot{x} = \dot{f}_L^2 x + \ddot{f}_L y + 2\dot{f}_L\dot{y} + \mu \Big/ r_t^2 - \mu(r_t + x) \Big/ r_c^3 + f_x \\
\ddot{y} = -\ddot{f}_L x + \dot{f}_L^2 y - 2\dot{f}_L\dot{x} - \mu y \Big/ r_c^3 + f_y \\
\ddot{z} = -\mu z \Big/ r_c^3 + f_z
\end{cases} \tag{3}$$

where, $f = \Delta f_d + a_c - a_t$.

The above formula can be linearized [8], and the approximate expression is

$$\begin{cases}
\ddot{x} - 2\dot{f}_L\dot{y} - \dot{f}_L^2 x - \ddot{f}_L y - 2\mu x \Big/ r_t^3 = f_x \\
\ddot{y} + 2\dot{f}_L\dot{x} - \dot{f}_L^2 y + \ddot{f}_L x + \mu y \Big/ r_t^3 = f_y \\
\ddot{z} + \mu z \Big/ r_t^3 = f_z
\end{cases} \tag{4}$$

3 Design of AREKF Filtering Algorithm

Combined with the spacecraft dynamics model, a navigation filter scheme based on visual measurement is designed to quickly estimate the target orbit information [9–11].

a) The simulation model of ultra-close range relative motion tracking and control is established (Fig. 3).

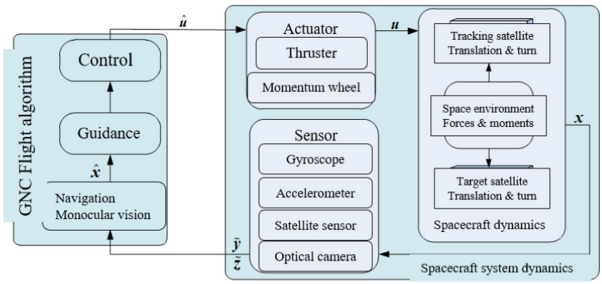

Fig. 3. Spacecraft ultra-close-range relative motion tracking and control system diagram

The actuator, sensor and their error models are constructed [12, 13], the tracking acquisition alignment scheme is designed, the guidance control model and actuator configuration are derived, and the dynamic model of navigation state is established

$$\dot{\mathbf{x}} = \begin{bmatrix} \dot{\boldsymbol{x}}_T \\ \dot{\boldsymbol{x}}_C \\ \dot{\boldsymbol{x}}_P \end{bmatrix} = \begin{bmatrix} \dot{\boldsymbol{r}}_t \\ \dot{\boldsymbol{v}}_t \\ \dot{\boldsymbol{\theta}}_t^t \\ \dot{\boldsymbol{\omega}}_t^t \\ \dot{\boldsymbol{r}}_c \\ \dot{\boldsymbol{v}}_c \\ \dot{\boldsymbol{\theta}}_c^c \\ \dot{\boldsymbol{\beta}}_a^c \\ \dot{\boldsymbol{\beta}}_\omega^c \\ \dot{\boldsymbol{\varepsilon}}_s^s \\ \dot{\boldsymbol{\varepsilon}}_o^o \end{bmatrix}_{33\times 1} \quad \mathbf{f}(\mathbf{x}) = \begin{bmatrix} \boldsymbol{v}_t \\ \boldsymbol{g}_t + \boldsymbol{a}_t \\ \left(\boldsymbol{\omega}_t^t - \hat{\omega}_t^t\right) - \hat{\omega}_t^t \times \boldsymbol{\theta}_t^t \\ \boldsymbol{I}_t^{-1}\left[\boldsymbol{\tau}_g^t - \boldsymbol{\omega}_t^t \times \left(\boldsymbol{I}_t \boldsymbol{\omega}_t^t\right)\right] \\ \boldsymbol{v}_c \\ \boldsymbol{g}_c + \boldsymbol{T}\left(\hat{\boldsymbol{q}}_{c\to i}\right)\left(\tilde{\boldsymbol{a}}_c^c - \boldsymbol{\beta}_a^c\right) \\ \hat{\boldsymbol{\beta}}_\omega^c - \boldsymbol{\beta}_\omega^c - \left(\tilde{\boldsymbol{\omega}}_c^c - \hat{\boldsymbol{\beta}}_\omega^c\right) \times \boldsymbol{\theta}_c^c \\ -\boldsymbol{\beta}_a^c / \tau_{\beta a} \\ -\boldsymbol{\beta}_\omega^c / \tau_{\beta\omega} \\ -\boldsymbol{\varepsilon}_s^s / \tau_{\varepsilon \mathrm{s}} \\ -\boldsymbol{\varepsilon}_o^o / \tau_{\varepsilon \mathrm{o}} \end{bmatrix}_{33\times 1} \tag{5}$$

b) A robust adaptive filtering method is proposed for uncooperative targets

The recursion formula is as follows

$$\hat{\boldsymbol{X}}(k, k-1) = \boldsymbol{\Phi}(k, k-1)\hat{\boldsymbol{X}}(k-1, k-1) \tag{6}$$

$$\boldsymbol{P}(k, k-1) = \boldsymbol{\Phi}(k, k-1)\boldsymbol{P}(k-1, k-1)\boldsymbol{\Phi}^T(k, k-1) + W(k-1) \tag{7}$$

$$\tilde{z}(k) = z(k) - \boldsymbol{H}(k)\hat{\boldsymbol{X}}(k, k-1) \tag{8}$$

$$\boldsymbol{P_Y}(k) = \boldsymbol{H}(k)\sum(k, k-1)\boldsymbol{H}^T(k) + \boldsymbol{V}(k) \tag{9}$$

$$\boldsymbol{K}(k) = \sum(k, k-1)\boldsymbol{H}^T(k)\boldsymbol{P_Y}^{-1}(k) \tag{10}$$

$$\hat{\boldsymbol{X}}(k, k) = \hat{\boldsymbol{X}}(k, k-1) + \boldsymbol{K}(k)\tilde{z}(k) \tag{11}$$

$$\boldsymbol{P}(k, k) = (\sum{}^{-1}(k, k-1) + \boldsymbol{H}^T(k)\boldsymbol{V}^{-1}(k)\boldsymbol{H}(k))^{-1} \tag{12}$$

$$\sum(k, k-1) = (\boldsymbol{P}^{-1}(k, k-1) - \gamma^{-2}N(k)N(k))^{-1} \tag{13}$$

where, $\sum(k, k-1) = S(\boldsymbol{P}(k, k-1)), N(k) = \gamma(\boldsymbol{P}^{-1}(k, k-1) - \varepsilon^{-2}\boldsymbol{I})^{1/2}$.

In order to enhance the flexibility of introducing robustness, AREKF algorithm provides a gain scheduling operator with adaptive switching structure

$$\sum(k, k-1) = \begin{cases} (\boldsymbol{P}^{-1}(k, k-1) - \gamma^{-2}N(k)N(k))^{-1}, & \overline{\boldsymbol{P}}_Y(k) > \alpha\boldsymbol{P}_Y(k) \\ \boldsymbol{P}(k, k-1), & \overline{\boldsymbol{P}}_Y(k) \le \alpha\boldsymbol{P}_Y(k) \end{cases} \tag{14}$$

4 Simulation Analysis

In this paper, The main parameter settings are as follows:

1) Parameter setting of two spacecrafts
$\boldsymbol{r}_c = [5115213.213 \quad -3997892.911 \quad -334532.798]^T m$,
$\boldsymbol{v}_c = [4819.712 \quad 6170.435 \quad -70.256]^T m/s$.
$\boldsymbol{r}_t = [5114215.813 \quad -3996543.324 \quad -334956.567]^T m$,
$\boldsymbol{v}_t = [4817.578 \quad 6170.435 \quad -70.123]^T m/s$.

At this point, the tracking star in the orbital coordinate system is 150 m behind the target in the direction of the orbit, 50 m behind in the radial direction, and the relative velocity with the tracking satellite is 0.

The inertia matrix of the tracking star and the target star is as follows

$$\boldsymbol{I_t} = \boldsymbol{I_c} = \begin{bmatrix} 4000 & 0 & 0 \\ 0 & 5000 & 0 \\ 0 & 0 & 1000 \end{bmatrix} kg \cdot m^2$$

$\theta_{t0} = [-5° \ -5° \ -5°]^T$, $\theta_{c0} = [5° \ 5° \ 5°]^T$, and the rotation order is 321, then
$\boldsymbol{q}_{i\to t} = \left[0.6231 \ 0.3112 \ 0.2569 \ 0.6748\right]^T$, $\boldsymbol{q}_{i\to c} = \left[0.6739 \ 0.3374 \ 0.3414 \ 0.5638\right]^T$
$\boldsymbol{\omega}_t^t = \boldsymbol{\omega}_c^c = [-0.006 \quad 0.068 \quad 0.006]^T \ ^o/s$
Suppose that three feature points are extracted from the target satellite.

$\boldsymbol{r}_{F1}^{t} = [-0.6\ \ 0.0\ \ 0.0]^{\mathrm{T}}m$, $\boldsymbol{r}_{F2}^{t} = [-0.7\ \ 0.1\ \ 0.0]^{\mathrm{T}}m$, $\boldsymbol{r}_{F3}^{t} = [-0.7\ \ 0.0\ \ 0.3]^{\mathrm{T}}m$.

$\boldsymbol{r}_{\mathrm{o}}^{c} = [1.1\ \ 0.1\ \ 0.0]^{\mathrm{T}}m$, $\boldsymbol{r}_{dock}^{t} = [-0.8\ \ 0.0\ \ 0.0]^{\mathrm{T}}\mathrm{m}$, $\boldsymbol{r}_{attach}^{C} = [1.0\ \ 0.0\ \ 0.0]^{\mathrm{T}}\mathrm{m}$.

The maximum acceleration of the thruster on the target satellite is 2 mm/s^2. Track the maximum acceleration of the thruster on the satellite is 5 mm/s^2.

2) Error parameter (Tables 1, 2 and 3).

Table 1. Initial state error (3σ)

Parameter name		Values
Navigation errors of attitude and attitude angular velocity of target satellite	Per axis	0.3 rad, 0.3 mrad/s
Target positioning and speed deviation	Per axis	30 m, 0.3 m/s
Navigation errors of attitude and attitude angular velocity of tracking satellite	Per axis	0.003 rad, 0.003 mrad/s
Tracking satellite position and speed navigation error	Per axis	30 m, 0.3 m/s

Table 2. Spacecraft dynamics disturbance (3σ)

Parameter name		Values
Rotation interference error	Per axis	0.002 mrad/s/$\sqrt{\mathrm{s}}$
Translational interference error	Per axis	0.05 mm/s/$\sqrt{\mathrm{s}}$

3) Result analysis

Under the condition of open-loop control, the relative location, speed and posture between the tracking satellite and the target can be estimated accurately. After a period of filtering, it is quickly corrected, and the error curve is basically stable after 500 s. The final relative position estimation error standard deviation is 0.4 m (3σ), and the standard deviation of relative posture estimation error is 0.6° (3σ). As shown in Fig. 4.

4) Under the closed-loop control condition, After about 300 s, the attitude of the tracking satellite is basically adjusted to be consistent with that of the target satellite, and the final relative attitude control accuracy is within 1°, as shown in Fig. 5:

5 Conclusion

Based on the disturbance of relative motion uncertainty and measurement error under maneuvering conditions, The attitude-orbit coupling dynamics model of non cooperative goal is established, Based on the principle of AREKF filter, a fast method for estimating

Table 3. Sensor error

Parameter name		Values
Gyroscope error	Drifting error	5.0 deg/hr/axis
	Sensitivity	200 ppm/axis
	Misalignment error	2 mrad/axis
	Angle random walk	0.03 mrad/$\sqrt{s}$
	Slope random walk	5×10^{-7} mrad/s/$\sqrt{s}$
Accelerometer error	Drift error	1×10^{-4} m/s^2/axis
	Sensitivity	200 ppm/axis
	Misalignment error	0.01 mrad/axis
	Random walk	2×10^{-4} m/s/$\sqrt{s}$
Satellite sensor error	Misalignment error	1.1 mrad/axis
	Measurement noise	0.2 mrad/axis
	Sampling rate	1 s
Optical camera deviation	Misalignment error	1.1 mrad/axis
	Measurement noise	0.2 mrad/axis
	Sampling rate	1 s

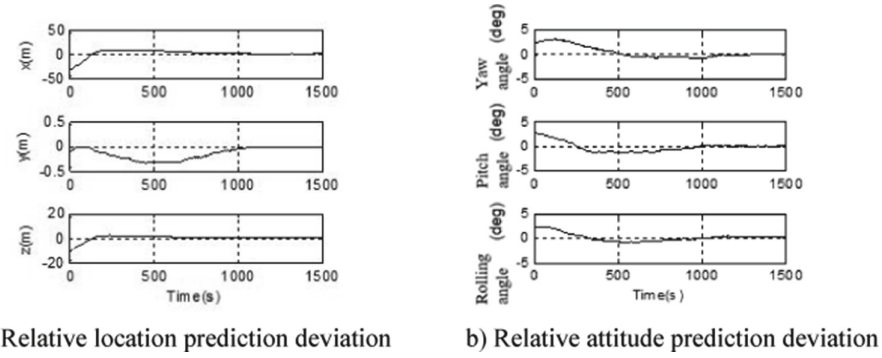

Fig. 4. Deviation curve of relative pose estimation under open loop condition

the orbit information of non cooperative target is proposed. Simulation results indicate that this algorithm is able to accurately estimate relative location, speed and posture of two satellites.

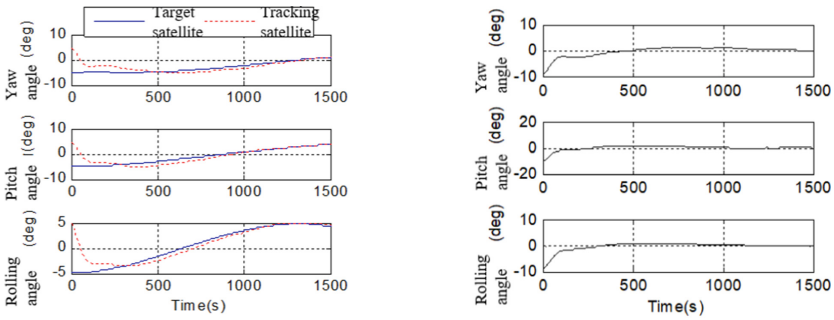

Fig. 5. Relative pose deviation curve under open loop condition

References

1. Davis, J.P., Mayberry, J.P., Penn, J.P.: On-orbit servicing: inspection, repair, refuel, upgrade, and assembly of satellites in space. The Aerospace Corporation, pp. 1–14. Report (2019)
2. Du, X.D., Liang, B., Xu, W.F.: Pose measurement of large non-cooperative satellite based on collaborative cameras. Acta Astronaut. **68**, 2047–2065 (2011)
3. Angel, F.A., Ou, M., Khanh, P.: A review of space robotics technologies for on-orbit servicing. Prog. Aerosp. Sci. **68**, 1–26 (2014)
4. He, Y.Z., Wei, C.L., Tang, L.: A survey on space operations control. Aerosp. Control Appl. **40**(1), 1–8 (2014)
5. Wang, X.H.: Space on orbit service technology and its development status and trend. Satell. Netw. 70–76 (2016)
6. Geller, D.: Analysis of the relative attitude estimation and control problem for satellite inspection and orbital rendezvous. J. Astronaut. Sci. **55**(2), 195–214 (2007)
7. Howard, D.C.: Orbital Mechanics for Engineering Students. Elsevier's Science & Technology, Oxford (2005)
8. Bong, W.: Space vehicle dynamics and control. In: Proceedings of the AIAA Education Series, Virginia (1998)
9. Liang, B., Du, X.D., Li, C.: Advances in space robot on-orbit servicing for non-cooperative spacecraft. Robot **24**(2), 242–265 (2012)
10. Xiong, K., Zhang, H., Liu, L.: Adaptive robust extended Kalman filter for nonlinear stochastic systems. IET Control Theory Appl. **2**(3), 239–250 (2008)
11. Segal, S., Carmi, A., Gurfifil, P.: Stereovision-based estimation of relative dynamics between noncooperative satellites: theory and experiments. IEEE Trans. Control Syst. Technol. **22**(2), 568–584 (2014)
12. Pesce, V., Lavagna, M., Bevilacqua, R.: Stereovision-based pose and inertia estimation of unknown and uncooperative space objects. Elsevier's Space Res. 1–16 (2016)
13. Ghiasi, A.R., Ghavifek, A.A.R., Shabbouei Hagh, Y.: Designing adaptive robust extended Kalman filter based on Lyapunov-based controller for robotics manipulators. In: 6th International Conference on Modeling, Simulation, and Applied Optimization, pp. 1–6. IEEE, Istanbul (2015)